IEEJ Journal of Industry Applications
Vol.8 No.4 pp.677–684 DOI: 10.1541/ieejjia.8.677

Paper

Loss Characteristics of Input-Series Output-Parallel SiC DC-DC Converter Used in Auxiliary Power Systems

Xianjin Huang* Non-member, Juan Zhao*a) Non-member
Fenglu Li* Non-member, Fei Lin* Non-member

(Manuscript received Aug. 30, 2018, revised Feb. 25, 2019)

With regard to the auxiliary power systems used in public transport such as hybrid bus, trolleybus, light rail trams, and subways, riding the weight and volume of the power equipment need to be reduced in order to accommodate more passengers or provide a more comfortable space. A converter with a higher capacity density, smaller volume, and lower weight was developed to improve the vehicle layout design and transport capability. With advantages such as faster switching frequency, lower power losses, and higher working temperature, silicon carbide metal-oxide-semiconductor field-effect transistor (SiC MOSFET) devices can be used to promote the operation of auxiliary power converters. In most of the metro trains in China, such as Beijing, Shanghai, and Guangzhou, the power supply line is at a level of DC 1500 V. However, 3300 V SiC devices are rarely available in the market, series SiC MOSFETs are mostly available at levels of 600 V to 1200 V. In this research, a cascaded full-bridge topology with input-series output-parallel (ISOP) connected converter adapting 1700 V/300 A SiC MOSFET is proposed. An improved input voltage sharing control method is applied to improve the system rapidity and stability of the ISOP converter. The working characteristics, device losses, and system efficiency of a phase-shifted full-bridge (PSFB) converter with ISOP topology based on 1700 V/300 A SiC MOSFET are studied. Aiming at the application to auxiliary power systems, the other two types of converter topologies are also analyzed. The 1700 V/300 A (silicon-based insulated gate bipolar transistor) Si IGBT PSFB converter with ISOP topology and the 3300 V/400 A Si IGBT single unit PSFB converter are investigated of the control, weight, losses, efficiency, cost, and structure complexity. Simulation and experiment show the application of SiC devices exerting a positive effect on the volume reducing, weight decreasing and efficiency increasing.

Keywords: ISOP PSFB converter, loss characteristics, SiC MOSFET

1. Introduction

There are strict standards on the weighty and volume of auxiliary power system applied to the tram, light railway transit (LRT) and metro train. Higher capacity density, smaller volume and slighter weight of the converter are beneficial to the vehicle layout design and transport capability. The power level of the latest domestic metro vehicle auxiliary inverter power system is generally 150 kW. In most Chinese cities like Beijing, Shanghai, Wuhan and Shenzhen, the subway power supply line was direct current power (DC) 1500 V system. The vehicle auxiliary power supply was consisted by DC 700 V bus, DC 110 Vbattery charger, three phase 380 Vac inverter and DC 24 V signal power module. The power density, volume and weight can be improved by the output filter and the transformer isolation. So the additional high-frequency DC-DC link is often used, which changes the output side industrial frequency transformer into the high-frequency transformer. The loss characteristics of the converter after increasing an additional high-frequency DC-DC link has been studied in Ref. (1). The different topologies of the converter fore-stage circuit has been studied in Refs. (2)– (5). The increasing topologies of the fore-stage circuit can improve the converter weighty, volume and power density, but it also increases the cost of the devices and the risk of failure. There are 2 methods to improve the performance of the DC-DC converter, one is to improve the circuit topology, the other is to enhance the operating frequency, including the directly increase of the frequency and the use of new devices. An improved parallel circuit applied to the auxiliary power system has been investigated in Ref. (6). A train auxiliary power supply system based on PQ droop control algorithm has been designed in Ref. (7). There was a modular redundant design on the DC-DC converter to reduce the single module power [(8)]. The DC-DC converter with SiC MOSFET has been analyzed for the system loss and efficiency [(9)(10)].

Soft-switching is the most common way to increase the switching frequency of the Si-based devices, thereby reducing device losses and ensuring system efficiency. Many literatures have carried out related research based on a certain topology, including soft-switching circuit stability, soft-switching implementation and the efficiency of the circuit like introduced in Refs. (11)– (15). Wide bandgap devices bring the characteristics of high-frequency and low-loss to enhance the circuit performance. Many circuits with wide bandgap devices can be implemented under hard switches, reducing the design requirements for circuit parameters and

a) Correspondence to: Juan Zhao. E-mail: 767129857@qq.com
* Beijing Jiaotong University
No.3 ShangYuan Village, Haidian District, Beijing City, China

simplifying control algorithms. The application of SiC MOSFETs in aeronautical static converters has been studied in Ref. (16). Due to the commercialization process in the industry, the present common module of the SiC devices is only at 1700 V level, which also limits the applications of the SiC devices in the subway auxiliary power supply system.

The input series output parallel (ISOP) phase shifted full bridge (PSFB) zero voltage switch (ZVS) DC-DC converter circuit topology using 1700 V SiC MOSFET suitable for DC 1500 V power supply is studied in this paper. The converter uses two power modules input series output parallel. Each single power module uses full bridge structure which can achieve high-frequency isolation and phase-shifted control. The control method of the ISOP double bridge system is studied, and the input voltage and output current sharing are guaranteed by the improved input voltage sharing control algorithm. With two-level converter using the traditional 3300 V Si devices and ISOP double bridge circuit structure using the ordinary 1700 V Si devices, the control characteristics, operating principles, loss and efficiency characteristics of the three structures are compared. Finally, the relationship between the loss and the operating frequency of the ISOP PSFB converter with SiC MOSFET is studied, and the design parameters of the converter in auxiliary power supply system are determined. The feasibility of the scheme is verified by simulation and experiment results.

2. DC-DC Converter for Auxiliary Power Supply

2.1 PSFB SiC DC-DC Converter The converter in this paper is for 1500 V powered auxiliary power system (APS). There are generally two types to supply power to APS: centralized power supply and distributed power supply [17]. There is also one structure such as the Guangzhou metro line 2 in Fig. 1 [18].

T_c stands for trailer and M_p stands for motor train in the Fig. 1. One T_c and two M_p form a power supply unit. The power supply is 1500 V high voltage DC bus. FV represents lightning arrester. Each high-voltage box is equipped with a 3-position knife switch, which can be switched in three modes: pantograph position, grounding position and workshop power supply. F stands for fuse. There is an APS3 in carriage T_c. There is an APS2 and a traction inverter in M_{p2} powering the engine M3 and M4. There is an APS3 and a traction inverter in M_{p1} powering the engine M1 and M2.

The APS2 and APS3 structures in the power supply system of Fig. 1 are like Fig. 2 shows.

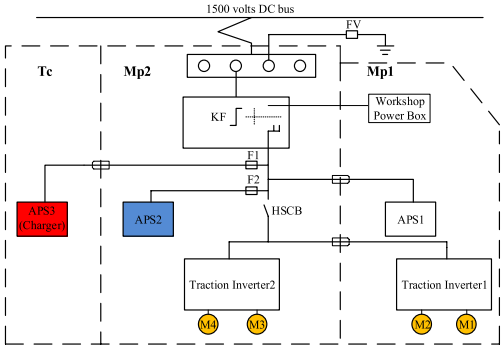

Fig. 1. Guangzhou metro line 2 power supply system

As Fig. 2 shows, APS3 (APS with charger) often concludes two stage circuits. The pre-stage circuit is a high power high voltage DC-DC converter which is supplied by the DC 1500 V bus. In general, the output is DC 600 V or DC 700 V and the power is greater than 50 kW. The rear-stage circuit concludes three parts. The first is a converter that charges the 110 V battery charger. The power is generally 15 kW. The second is a DC 24 V or DC 48 V power supply module which supplies the control unit power. The power is generally not more than 500 W. The last is a buck converter which supplies DC 24 V for control circuit.

The DC-DC converter can convert the DC 1500 V input into the DC 700 V output by bridge circuit, step-down transformer, diode rectifier and the LC filter. The half-bridge circuit can supply the DC 110 V with the DC 700 V input. The three-phase inverter generally uses bridge circuit topology, which converts the DC 700 V input into the AC 380 V output.

The high-voltage high-power DC-DC converter uses two-level structure in common. For DC 1500 V power supply, 3300 V IGBT can meet the requirements. The **conventional** DC-DC converter structure is IGBT phase-shifted full bridge converter. For 1700 V SiC switching devices, the traditional two levels cannot meet the voltage pressure requirements. In Fig. 3, there are two PSFB converters in series or parallel structure.

The input-series structure can reduce the voltage stress of the devices, and the output-parallel structure can reduce the current stress of the output rectifier. With the input-series structure, 1700 V SiC MOSFET can be used in the full bridge structure. There are two input capacitors and output filter

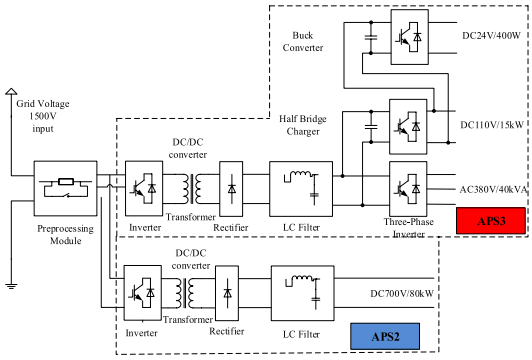

Fig. 2. Structure of APS2 in Mp2 and APS3 in Tc

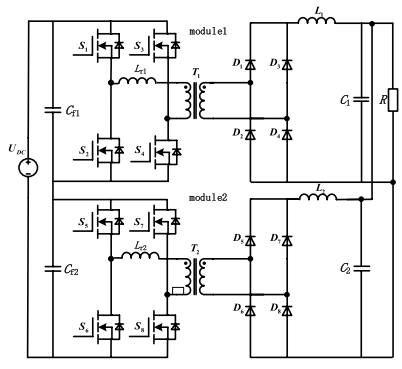

Fig. 3. SiC MOSFET ISOP PSFB converter (DC-DC converter)

Table 1. PSFB converter operating mode of one half period

i_{Lr}	Pulse distribution	Conduction devices
>0	S_4(S_1 OFF)	S_1,S_4,D_1,D_4
>0	S_4	S_4,D_1,D_4
>0	S_4,S_2	S_4,SD_2,D_1,D_4
<0	S_2	SD_2,SD_3,D_1,D_2,D_3,D_4
<0	S_2,S_3	SD_2,SD_3,D_1,D_2,D_3,D_4
<0	S_2,S_3	S_2,S_3,D_1,D_2,D_3,D_4
<0	S_2,S_3	S_2,S_3,D_2,D_3

inductors and capacitors. And the resonant inductor is also given to make the switching realize ZVS.

Each power module is in full bridge structure and phase-shifted control in Fig. 3. The two full bridge modules share the input voltage so that the 1700 V switching devices can meet the 1500 V power supply requirements. And the improved input voltage sharing control is used in the ISOP structure to ensure the input voltage sharing and the output current sharing.

For a single full-bridge DC-DC converter, phase-shifted control is used to achieve ZVS. In phase-shifted control, the phase of S_1 is ahead of S_4 and the phase of S_2 is ahead of S_3, so it is often said that S_1 and S_2 make up the leading leg, and S_3 and S_4 make up the lagging leg. When there is not a shift-phase between the leading leg and the lagging leg, the primary side of the transformer obtains the largest volt-second product [19], allowing the converter to obtain the maximum output voltage. When the shift-phase is equal to or greater than 180°, the primary side voltage of the transformer is 0 and there will be no output. In the dead zone, the resonant inductance L_r, the filter conductor L_f and switching device junction capacitance resonance to open the switches of the leading leg before the $V_{ds}(V_{ce})$ voltage drop to zero to achieve ZVS. Besides, the resonant inductance L_r and its switching device junction capacitance resonance to open the lagging leg switches before the $V_{ds}(V_{ce})$ drop to 0 to achieve ZVS, too. The PSFB converter operating mode of one half period is summarized as Table 1.

Table 1 shows one half period of a PSFB converter operation mode, and the last half period is the similar. *S*n represents the switching devices of the full bridge in Fig. 4. *SD*n represents the corresponding switching devices body diode. *D*n is for the diode of the rectifier. i_L is the current flowing through the resonant inductance L_r. Similar to the working principle of a phase-shifted full-bridge module, the two phase-shifted full-bridge module input series output parallel structure works the same way.

Figure 4 shows the converter waveforms during the different operation modes. The pulses of switches, the shifted phase between the switches of the leading leg and the lagging leg, the current flowing through L_r, the voltage V_{AB} between the two midpoint of H bridge, the second side voltage of the transformer V_{T2}, the output voltage V_o are shown here. As it was also showed how the voltage V_{AB} and the current flowing through L_r change in the dead time. The dotted curve of the second side voltage of the transformer V_{T2} shows the duty cycle lost.

The drive pluses of module 2 are all lagged by module 1 a degree θ. The output current is the sum of the current of module 1 and the current of module 2. Module 1 is operated as the same as one PSFB converter like the Fig. 4 shows. In

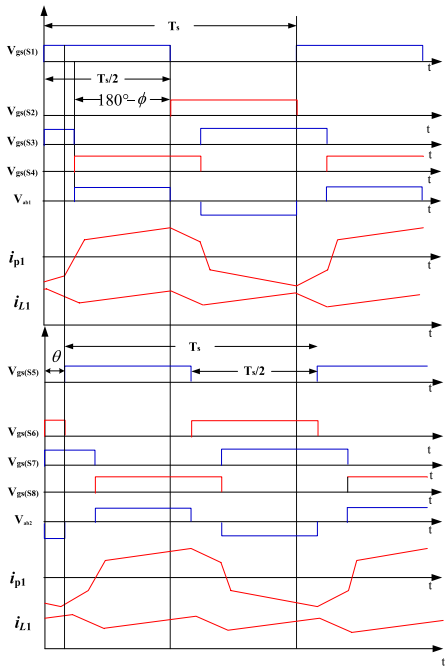

Fig. 4. ISOP PSFB converter operation waveforms

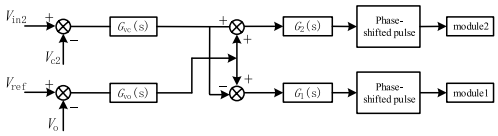

Fig. 5. Commonly used input voltage sharing control

general, in order to reduce the loss of the converter, there will be a phase between the two modules as the degreeθ. So the output current ripple will be canceled out when the currents of the two modules are superimposed. As you can see, the i_{L1} and i_{L2} are staggered.

The blue lines often show the voltages and the red lines often show the current. The dead time of the switches is ignored to briefly describe how the converter works. But one PSFB module actual working process is as the Fig. 4 shows. For the ISOP PSFB converter, the input current sharing and the output voltage sharing are very significant control indicators. If the two aims can be achieved, the converter can be operated stably. So, we will discuss the control method and its influences to the converter stability and loss.

2.2 ISOP PSFB Converter Control Due to the commercialization process in the industry, the present common module with the SiC devices is only at 1700 V level. In order to use the 1700 V SiC devices well, two power modules in series structure in the input which can ensure the voltage pressure is widely used. And the parallel structure in the output makes that one power module only needs meeting the half of the output current requirement. But there is a problem caused by the ISOP structure that is the input voltage and the output current may not be shared equally by the two modules.

In order to achieve the goal of input voltage sharing and output current sharing. There is a normal control method as shown in Fig. 5.

The amplitude of V_{in2} is half the input voltage U_{dc} in Fig. 3. V_{c2} is for the voltage of the capacitor C_{f2}. V_{ref} is the output

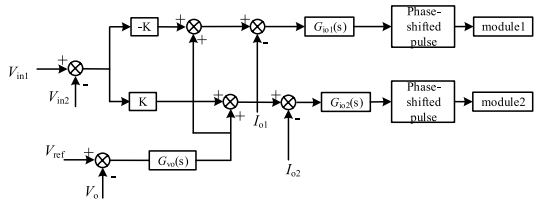

Fig. 6. An improved input voltage sharing control

voltage reference value. G(s) is for the PI regulator of the various control loops. There are two control loops coupling in the common control method. The input voltage equalization loop and output current loop are coupled to ensure voltage and current sharing. If the control system can control the input voltage and the output current sharing, so the system can work stably [20]. So the commonly used input sharing control method is proposed in Fig. 5. As there is no current loop in the control system, the response of the system is slow.

Based on the commonly used input voltage sharing control method, in order to improve the rapidity and stability of the system, an improved input voltage sharing control method is proposed in Fig. 6.

There is a common output voltage loop in Fig. 6, individual average current mode inner current loop, whose references are adjusted by individual input voltage loops. And the difference between the input voltages of the two modules after multiplying a gain K, respectively plus or minus the value after the outside voltage loop regulator and then conducts as the output of the input voltage loops. Output control pulses are regulated by the inner current loop regulator output to control the converter output.

The two voltage outer loops respectively ensure that the input voltage is equally divided and the output voltage is stable, and the inner current loop ensures the equalization of the output current. In the case of a suitable parameter setting, due to the inclusion of the inner current loop, the system's rapidity is improved and the stability of the system is also improved.

3. Simulation and Loss Calculation

In order to verify that the circuit topology can meet the specifications and requirements of the auxiliary converter. The ISOP SiC DC-DC converter simulation model are built by PSIM. The control pulses and the voltages and currents of the switches are shown in Fig. 7.

The coordinates of each vertical axis are shown on the upper left side of the waveform, and each of the four sets of waveforms shares a time horizontal axis. As the Fig. 7 shows, the top waveforms show the turn on pluses of the eight switches of the two modules. And the below waveforms show the switching voltage and current waveforms of the two modules leading and lagging arms respectively. It can be seen that the waveforms of the four switches are all started to rise after the voltage drops to zero so that it realizes ZVS. The output voltage is obtained and kept stable at 700 V.

There are other two circuits to obtain the DC-DC converter objectives in auxiliary power system and their simulation models are built by PSIM. The conventional converter is 10 kHz PSFB converter using IGBT and the waveforms are shown in Fig. 8.

As the figure shows, both IGBT1 and IGBT4 of the lagging leg achieved ZVS, and the output voltage is obtained and kept stable at 700 V. The output voltage ripple is smaller than 1.0 V.

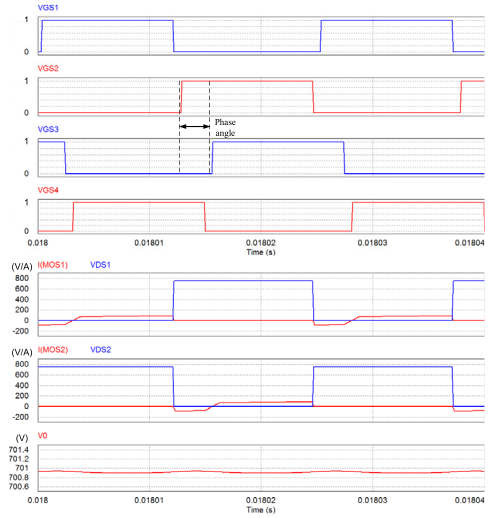

Fig. 7. 40 kHz SiC MOSFET ISOP PSFB Simulation waveforms

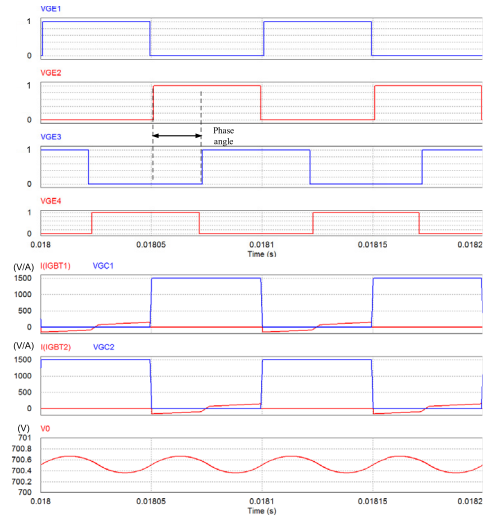

Fig. 8. 10 kHz IGBT PSFB Simulation waveforms

The PSIM model simulation waveforms of ISOP PSFB converters with Si IGBT are given as Fig. 9.

It can be seen that both the leading and the lagging arms realized ZVS. The phase angles of each converter are different, and all of the output ripples are smaller than 1 V. So all the converters can work normally and reach control indicators.

3.1 Conduction Loss The first converter uses FF400R33KF2C IGBT of Infineon. And most of the losses are conduction loss P_{con}, switching loss P_s, rectifier loss P_{rec}, circulation loss, P_{cir} transformer loss P_t and LC filter loss P_{Lf}. The formulas of the losses Calculation are as follows.

$$P_{con} = f_s \int_0^{T/2} U_{ce}(t) I_e(t) dt \cdots\cdots\cdots\cdots\cdots\cdots (1)$$

In general, the conduction loss is calculated as formula (1) if there is the working waveforms. But in order to quickly and easily estimate the conduction loss, we will use data from the datasheets to estimate the value. So the conduction loss is

$$P_{con(MOS)} = I_{rms}{}^2 R_{ds(on)} D_s \cdots\cdots\cdots\cdots\cdots\cdots (2)$$

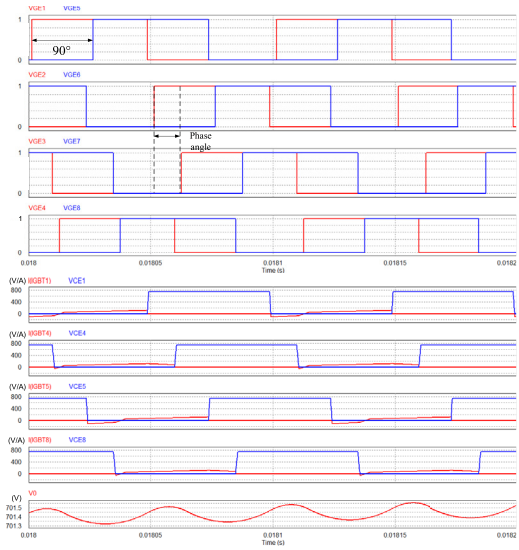

Fig. 9. 10 kHz Si IGBT ISOP PSFB Simulation waveforms

$$P_{con(IGBT)} = I_{rms} V_{ce(i=i_{rms})} D_s \cdots\cdots (3)$$

In the formula, I_{rms} is the RMS value of the current flowing through the devices. $R_{\mathrm{ds(on)}}$ is on-state resistance of the devices. D_{s} is the effective duty cycle. $V_{\mathrm{ce}(i=i\mathrm{rms})}$ is the collector emitter voltage corresponding to the effective current flowing through the devices.

3.2 Switching Loss The switching energies at different power conditions are linearly related to the operating time voltage and current when we deal with high power applications. Based on the datasheet from manufacturer, the single switching energies E_{on} and E_{off} of the devices under specific test voltage and current is obtained. Then by correcting this loss value, we can get the switching losses through single switching energy and switching frequency.

$$P_s = P_{turn-on} + P_{turn-off} = f_s \left(E_{on} + E_{off}\right) \frac{V_d}{V_{dn}} \frac{I_d}{I_{dn}} \cdots\cdots (4)$$

In the formula, E_{on} and E_{off} are the loss of the switching turn on and turn off in the datasheet at the standard test condition, V_{dn} and I_{dn} are the voltage $V_{\mathrm{ce}}(V_{\mathrm{gs}})$ and current $I_{\mathrm{c}}(I_{\mathrm{d}})$ in the datasheet at the standard test condition, V_{d} and I_{d} are at the actual condition; and f_{s} is the switching frequency.

3.3 Rectifier Loss The rectifier loss concludes turn on loss and turn off loss (reverse recovery loss) of rectifier diodes D_1-D_4.

$$P_{Don} = D_D I_F V_F \cdots\cdots (5)$$

$$P_{Drr} = f_s E_{Drr} \frac{V_c}{V_{cn}} \frac{I_c}{I_{cn}} \cdots\cdots (6)$$

$$P_{rec} = P_{D-on} + P_{Drr} \cdots\cdots (7)$$

P_{Don} is the rectifier diode turn on loss, P_{Drr} is reverse recovery loss, D_{D} is the average duty cycle, V_{D} is the turn on diode voltage, I_{D} is the RMS value of the current flowing through the diode, R_{D} is equivalent resistance. E_{Drr} is reverse recovery loss.

From the conduction state to the reverse recovery state, U_{F} is turn-on voltage, I_{F} is turn-on current, t_{rr} is reverse recovery time, U_{RP} is reverse recovery peak voltage and I_{RP} is reverse recovery peak current. For many diodes datasheets, E_{Drr} is not given directly. But the I_{RP}, U_{RP} or the t_{rr} will be given in the datasheet. We can estimate its loss as follows.

$$E_{Drr} = 0.5 f_s U_{RP} I_{RP} t_{rr} \cdots\cdots (8)$$

The corresponding parameters will be given when the diode is shipped, so that the diode loss can be calculated.

3.4 Circulating Loss The circulating loss comes from the primary side full-bridge circuit during conduction or commutation. The charging and discharging of the switching capacitor can prevent the energy from being transmitted to the secondary side, and the energy flowing through the switching devices and the leakage inductance can be lost. It can be obtained by directly integrating according to the simulation result. The circulating loss of the full bridge is about the time t_1-t_4, the anti-parallel diode of the switching devices, and the filter inductance conduction.

$$P_{cir} = f_s \left(\int_0^{T_s} U_T(t) I_{Lr}(t) \right) dt + \int_{t1}^{t4} U_F(t) I_{Lr}(t)) dt \cdots\cdots (9)$$

$U_{\mathrm{T}}(t)$ is the turn on voltage of the anti-parallel diode, $U_{\mathrm{F}}(t)$ is the turn on voltage of the switching devices. The other one is caused by the DC resistance of transformer winding, and it does not only exist in the circulation process, but also exists in the process of the entire full-bridge circuit operation, so its calculation can be concluded in the transformer loss calculations.

$$P_{cir} = f_s \int_{t1}^{t4} U_F(t) I_{Lr}(t) dt \cdots\cdots (10)$$

As the formula shows, we only consider the loss from anti-parallel diode of the switching devices. It can also be estimated as follows.

$$P_{cir} = f_s U_{FN} I_{FN} \frac{I_F}{I_{FN}} \frac{U_F}{U_{FN}} \cdots\cdots (11)$$

So the circulation loss is obtained.

3.5 Magnetic Components Loss The loss of magnetic components is mainly composed of the core loss and winding loss.

$$P_{magnetic\ components} = P_{Fe} + P_{winding} \cdots\cdots (12)$$

The Core loss P_{Fe} can generally be calculated by the following formula.

$$P_{Fe} = k f_s^{\alpha} B^{\beta} V_e \cdots\cdots (13)$$

P_{Fe} is the core loss, B is the peak value of magnetic induction. k, α, β are constants, which depend on the grade of the material and they can be generally found from the manufacturers core manuals, V_{e} is for the volume of the core. The winding loss P_{winding} can be expressed as (neglecting AC resistance losses):

$$P_{winding} = {I_{rms}}^2 R_{coil} \cdots\cdots (14)$$

R_{coil} is the DC resistance of winding.

The transformer magnetic intensity peak value can be expressed as

$$B_T = \frac{U_o}{4 f_s A_e N_s} \cdots\cdots (15)$$

Where A_e is the effective magnetic field of the transformer. And the RMS value of the current flowing through the transformer is as follows.

$$I_{T\_rms} = \sqrt{f_s \int_0^{DT_s} \left(\frac{I_o}{k}\right)^2 dt \cdot R_{coil}} \cdots\cdots\cdots\cdots (16)$$

The loss value of the transformer P_t can be calculated by substituting the formula (15), (16) into the formulas (12)–(14) respectively.

The peak value of the AC magnetic intensity of the filter inductor L_f can be expressed as

$$B_{m\_Lf} = \frac{\mu_r \mu_o N_{Lf} \Delta I_o}{2 l_{e\_Lf}} \cdots\cdots\cdots\cdots\cdots\cdots (17)$$

Where ΔI_o is the output current pulsation, I_{Lf} is for the length of the effective magnetic circuit.

The current effective value of the filter inductor L_f is

$$I_{Lf\_rms} = I_o \cdots\cdots\cdots\cdots\cdots\cdots (18)$$

The loss of the filter inductor can be obtained by substituting the formula (17), (18) into the formulas (12)–(14) respectively.

4. Characteristics Comparison Analysis

According to the formulas, calculating the 10 kHz IGBT PSFB converter with FF400R33KF2C, the losses percentage of the rated power 80 kW is obtained. The proportion percentages of rated power P_{on}, P_t, P_{Lf}, P_{loop}, P_{rec}, P_s are 0.38%, 0.61%, 0.22%, 0.46%, 0.48%, 1.588% respectively.

4.1 Loss Characteristics Analysis of Three Converters

Every converter is designed in the best conditions in which switching frequency is suitable, ZVS is realized and the output meets the requirements. The rated power of each converter is 80 kW. The Si device operating frequency is 10 kHz. The SiC device operating frequency is 40 kHz. The main parameters and the switching devices of the converters are shown in the Table 2.

The middle one under the shadow is the proposed SiC MOSFET ISOP converter. All the converters are at the same rated power, but the switching frequency, transformer ratio, and the leakage inductance are different. The leakage inductance is designed according to their respective conditions.

According to Table 2, the loss and efficiency of each converter are calculated and is shown in Fig. 10.

In Fig. 10, for 40 kHz SiC MOSFET ISOP PSFB converter, the conduction loss P_{con} is the most, but all of the transformer loss P_t, the LC filter loss P_{Lf}, the circulation loss P_{cir} and the switching loss P_s are the least. For 10 kHz Si IGBT ISOP PSFB converter, the transformer loss P_t and the switching loss P_s are the most, and the total loss is the most. For 10 kHz Si IGBT PSFB converter, except the circulation loss P_{cir} is the most, the other losses are almost in the middle level. In all, the loss of the SiC MOSFET ISOP PSFB converter is the least, and the loss of the conventional Si PSFB converter is the most.

The above table compares the cost of the three converters under the main components, removing those common components. As can be seen from the table, the middle one under the shadow SiC MOSFET ISOP PSFB has the lowest loss,

Table 2. The main parameters of the converters

	switch type	P (kW)	fs (kHz)	Tn	Lr (uH)
Si PSFB	FF300R17KE4	80	10	1/1	31
SiC ISOP	CAS300M17BM2	80	40	1/1.4	4.65
Si ISOP	FF400R33KF2C	80	10	1/1.4	25.4

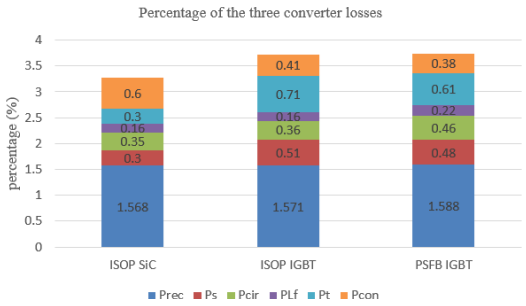

Fig. 10. Losses of the three kinds of converters

Table 3. Comparison of the three converter costs

	Specification	Si IGBT PSFB	SiC MOS ISOP PSFB	Si IGBT ISOP PSFB
Transformer	Ratio	1/1	1/1.4	1/1.4
	Lr	31uH	4.65 uH	25.4uH
	Size	170*260*200	145*240*170	170*300*200
	Weght	22kg	11kg	23kg
	Price(RMB)	3050	1900	3360
Drive module	Drive module price(RMB)	2*950=1900	4*1200=4800	4*500=2000
Switching	Switching	2*FF400R33KF2C	4* CAS300M17BM2	4* FF300R17KE4
	Price(RMB)	2*4500=9000	4*7000=28000	4*450=1800
Total cost	(RMB)	13950	34700	7160

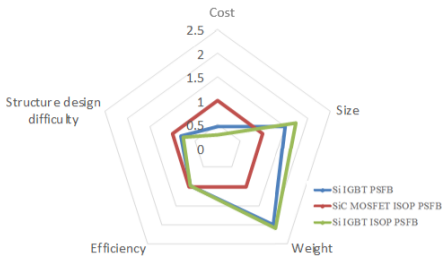

Fig. 11. Comparison of three converters

but its cost is also the most expensive. From this, it can be inferred that with the development of SiC devices, the performance will be improved. When the cost has been reduced, it is very appropriate to fully put into use.

In order to make a more detailed and profound comparison of the three converters, a radar diagram of the cost, size, weight, efficiency and structure design difficulty of the three converters is given as Fig. 11. The value of SiC MOSFET ISOP PSFB converter is taken as reference quantity 1, and the others are compared with it. As the figure shows, although the cost and structure design difficulty of the Si IGBT PSFB converter is the smallest, the size, weight and efficiency of the SiC MOSFET ISOP PSFB converter is the smallest. In all, SiC MOSFET does bring benefits to the converter.

4.2 Loss Characteristics Analysis of SiC ISOP Converter

In order to analyze the SiC switching devices advantages, the relationship between loss and frequency is studied and the system losses under full load and half load

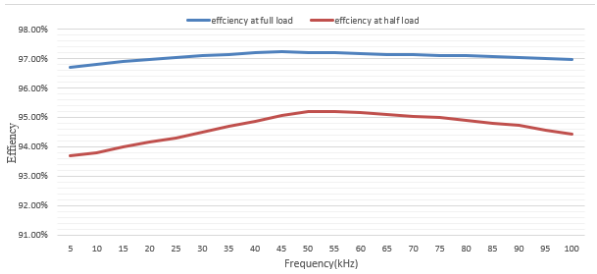

Fig. 12. Efficiency of SiC ISOP PSFB with frequency at full (half) load

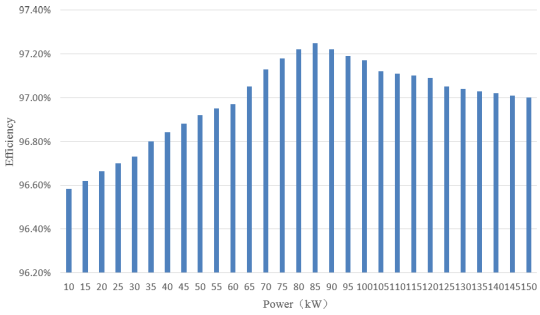

Fig. 13. Effciency of SiC ISOP PSFB with power

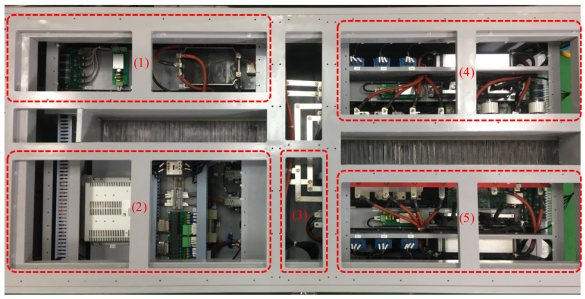

Fig. 14. SiC MOSFET ISOP PSFB converter experiment platform

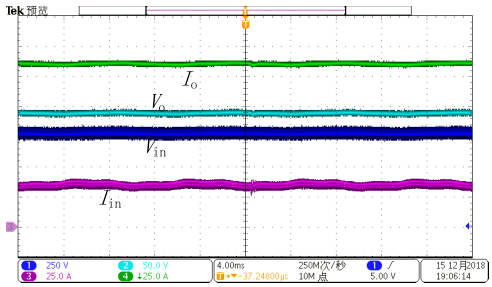

Fig. 15. Voltage and current waveforms of the switches

conditions are also given.

Figure 12 shows that the system efficiency with frequency at full load is almost reduced as the switching frequency increases. As the frequency increases, the resonant inductance increases with the calculation process, making the resonant frequency and switching frequency close to each other and the respective efficiency are at the highest. As the frequencies is up to 45 kHz, the efficiency is almost at its highest. So if using the SiC ISOP PSFB converter, 40 kHz frequency may be a good choice.

The system efficiency at half load is almost reduced as the switching frequency increases as shown in Fig. 12. As the frequencies is up to 50 kHz, the efficiency is almost at its highest. In all, if using the SiC ISOP PSFB converter, 40 kHz frequency may be a good choice.

The Fig. 13 above shows the loss of the converter at full load. The curve shows the efficiency is the lowest at 10 kW. The loss increases as the power increases during 10–80 kW. The efficiency decreases as the power increases after 80 kW, but the downward trend is relatively stable and there is not a very large change. A high efficiency will be obtained by choosing 80 kW as the rated power.

4.3 SiC MOSFET ISOP PSFB Converter at 25 kW

APS3 in Fig. 3 is built as Fig. 14 shows of a total 5 parts. Part (1) is inverter, part (2) is 110 V to 24 V power supply and interface board, part (3) is input and output interface section, part (4) is SiC MOSFET ISOP PSFB converter 1, part (5) is SiC MOSFET ISOP PSFB converter 2.

The experiment is for Part (4), the circuit structure is like Fig. 3 as a SiC MOSFET ISOP PSFB converter. The input voltage is 770 V, the dead time is 700 ns, the phase-shifted value is 1/4 switching cycle, the resonant inductor is 4.6 μH, the DC blocking capacitor is 30 μF, and the load is connected to the braking resistor cabinet. The dead time is 800 ns, the resistance load is adjusted to 1.6 Ω, and the duty ratio is

$$D = \frac{25 - 0.7 * 2}{25} * \frac{1}{2} = \frac{11.8}{25} \cdots\cdots\cdots\cdots\cdots\cdots (19)$$

Figure 15 shows input voltage, input current, output voltage, output current waveforms of the ISOP module.

As shown in the Fig. 15, after calculating the average value of each waveform with an oscilloscope, the converter efficiency at that power can be obtained.

$$\frac{189 * 134.5}{770 * 34.4} = 95.97\% \cdots\cdots\cdots\cdots\cdots\cdots\cdots\cdots (20)$$

The working power is about 26 kW. The calculation efficiency on the condition of 40 kW is 96.73%.

5. Conclusions

For the DC/DC converter in auxiliary power supply system of DC 1500 V input, the topology design of 1700 V SiC MOSFET ISOP PSFB circuit is proposed. The output of the DC/DC converter is stable by an input voltage sharing control. Compared with 3300 V Si IGBT PSFB converter and 1700 V Si IGBT ISOP PSFB converter, 1700 V SiC MOSFET ISOP PSFB converter meets the design requirements and the good operating conditions, the lowest loss 3.27% and the highest efficiency 96.73% are obtained according to the calculation results. And the efficiency of SiC MOSFET ISOP PSFB converter is 96.73% at 40 kW. The loss of each part under the rated condition of the converter still need further analysis.

Acknowledgment

The research is supported by “the Fundamental Research Funds for the Central Universities (2019JBM063)”. In this paper, the samples and test data were recorded with the strong support of CRRC QINGDAO SIFANG CO., LTD. We wish to express our heartfelt thanks to them.

References

(1) W. Zhou, S. Yang, X. Wu, and K. Sheng: "Optimal design of SiC MOSFETs for 20 kW DC-DC converter", 2017 29th International Symposium on Power Semiconductor Devices and IC's (ISPSD), Sapporo, pp.443–446 (2017)

(2) D. Sha, B. Li, W. Yuan, and Z. Guo: "An input series output parallel PSFB ZVS DC-DC converter based on load adaptation with auxiliary LC network and wide voltage range", Transactions of China Electro technical Society, Vol.36, No.13, pp.3558–3564+3374, DOI:10.13334/j.0258-8013. pcsee. 150160 (2016)

(3) S.R. Jang, S.H. Ahn, H.J. Ryoo, and G.H. Rim: "Novel high voltage capacitor charger for pulsed power modulator", 2010 IEEE International Power Modulator and High Voltage Conference, Atlanta, GA, pp.317–321 (2010)

(4) I.O. Lee and G.W. Moon: "Phase-Shift PWM Converter With a Wide ZVS Range and Reduced Circulating Current", *IEEE Transactions on Power Electronics*, Vol.28, No.2, pp.908–919 (2013)

(5) L. Zhao, H. Li, X. Wu, and J. Zhang: "An Improved Phase-Shift Full-Bridge Converter with Wide-Range ZVS and Reduced Filter Requirement", *IEEE Transactions on Industrial Electronics*, Vol.65, No.3, pp.2167–2176 (2018)

(6) K. Shen, J. Zhang, X. Yao, and J. Wang: "An improved Parallel Inverter for Train Auxiliary Power Supply System", *Transactions of China Electro technical Society*, Vol.28, No.5, pp.250–258 (2013)

(7) K. Shen, J. Zhang, and J. Wang: "Research on Auxiliary Power Supply System Based on PQ Droop Control Inverter Parallel Technology", *Transactions of China Electro technical Society*, Vol.26, No.7, pp.223–229 (2011)

(8) J. Wang, X. Chen, and L. Xiao: "Study on a Novel Input Parallel Output Series DC/DC Converter", Journal of Nanjing Normal University (Engineering & Technology Edition), Vol.12, No.1, pp.1–4 (2012)

(9) A.E. Awwad, N. Badawi, and S. Dieckerhoff: "Efficiency analysis of a high frequency PS-ZVS isolated unidirectional full-bridge DC-DC converter based on SiC MOSFETs", 2016 18th European Conference on Power Electronics and Applications (EPE'16 ECCE Europe), Karlsruhe, pp.1–10 (2016)

(10) S. Guo, P. Liu, R. Yu, L. Zhang, and A.Q. Huang: "Analysis and loss comparison of megahertz high voltage isolated DC/DC converters utilizing integrated SiC MOSFET module", 2016 IEEE 4th Workshop on Wide Bandgap Power Devices and Applications (WiPDA), Fayetteville, AR, pp.291–296 (2016)

(11) Z.L. Zhang, R. Yan, and Y. Luo: "A full-bridge ZVS converter applied to high power millimeter-wave gyrotron travelling wave tubes", 2016 IEEE International Conference on Microwave and Millimeter Wave Technology (ICMMT), Beijing, pp.167–169 (2016)

(12) P. O'Neill, J. Zhang, and W.G. Hurley: "A Phase-shift Full-Bridge ZVS DC/DC Converter for Wireless Charging of Electric Vehicles", 2015 50th International Universities Power Engineering Conference (UPEC), Stoke on Trent, pp.1–5 (2015)

(13) G.N.B. Yadav and N.L. Narasamma: "An Active Soft Switches Phase-Shift Full-Bridge DC–DC Converter: Analysis, Modeling, Design, and Implementation", in *IEEE Transactions on Power Electronics*, Vol.29, No.9, pp.4538–4550 (2014)

(14) I.O. Lee and G.W. Moon: "Phase-Shift PWM Converter With a Wide ZVS Range and Reduced Circulating Current", in *IEEE Transactions on Power Electronics*, Vol.28, No.2, pp.908–919 (2013)

(15) Y. Zhang, X. Guo, B. Guo, and Y. Bian: "The simulation and design of PSFB ZVS DC-DC converter based on Saber", 2014 IEEE Conference and Expo Transportation Electrification Asia-Pacific (ITEC Asia-Pacific), Beijing, pp.1–4 (2014)

(16) X. Ge, Z. Zhang, H. Cao, and S. Xie: "Applications of SiC MOSFET in Aeronautical Static Converter", Chinese Journal of Power Supply, Vol.14, No.4, pp.66–72, DOI:10.13234/j.issn. 2095-2805. 2016.4.66 (2016)

(17) Q. Zhao, Q. Liu, and M. Zeng: "Research and Development of Auxiliary Power System for Urban Rail Metro Vehicles", Locomotive Electric Drive, (01):52-57 (2012)

(18) C. Tang and C. Chen: "Analysis of Auxiliary Power Supply System for Urban Rail Transit Trains", Electric Switch, (01):12-15 (2008)

(19) C. Zhang, L. He, and Z. Zhang: "Summary of development of switching power supply technology", Microelectronics, (02):255-260+272. (2016)

(20) L. Cheng, X. Ruan, and T. Zhang: "Study on Control Strategy of DC-DC Converters Connected Input-Series Output-Parallel", Proceedings of the CSEE, No.22, pp.67–73 (2006)

Xianjin Huang (Non-member) received a Ph.D. in vehicle control and power from Bejing Jiaotong University, Beijing, China, in 2014. During 2012–2013, he was a visiting scholar of the Ecole Polytechnique Fédérale de Lausanne (EPFL), Switzerland. Currently, he is an Associate Professor of the School of Electrical Engineering, Beijing Jiaotong University. His research interests include electrical power supply of vehicle, power semiconductor's driver and high-efficiency converters.

Juan Zhao (Non-member) is studying at the School of Electrical Engineering, Beijing Jiaotong University. Her research is on electronic and electronic converters and high-frequency switching power supplies. At present, she is mainly doing research related to the subway auxiliary converter on power module serial-parallel control method and SiC MOSFET applications.

Fenglu Li (Non-member) is studying in the College of Electrical Engineering, Beijing Jiaotong University. His research direction is the application of SiC devices in power electronic converters. At present, he is studying the characteristics of SiC devices and the application advantages of SiC devices in rail transit auxiliary converters.

Fei Lin (Non-member) received his Ph.D. fromTsinghua University in 2004 and worked as a visiting scholar at Ohio State University in USA, 2009–2010. He is currently a professor at the School of Electrical Engineering at Beijing Jiaotong University and a doctoral tutor. His research direction is on Power Electronics and Power Drives. He has researched on urban rail permanent magnet traction drive system.